Second hidden triplet-singlet crossover of charged excitons in *n*-doped (Cd,Mn)Te/(Cd,Mg)Te in ultra-high magnetic fields

Y. Hirayama, E. Kojima, and S. Takeyama
Institute for Solid State Physics, University of Tokyo, Kashiwanoha 5-1-5, Kashiwa, Chiba 277-8581, Japan

G. Karczewski, T. Wojtowicz, and J. Kossut
Institute of Physics, Polish Academy of Science, Warsaw 02-668, Poland

(Received 11 July 2008; revised manuscript received 25 December 2008; published 30 March 2009)

We studied charged excitons realized in dilute magnetic semiconductor single-quantum wells (Cd,Mn)Te/(Cd,Mg)Te in high magnetic fields by photoluminescence (PL) measurements. We assigned two PL peaks which appeared in high magnetic fields as the singlet and the triplet charged excitons, respectively. It was shown from our PL analysis that the second hidden crossover between the triplet and the singlet charged excitons took place above 60 T. The singlet charged exciton transition was found to be the lowest energy in a higher magnetic side. Linear increase in the conduction-electron g factor with increasing magnetic field was deduced from the intensity ratio of two PL lines in magnetic fields up to 140 T.

DOI: 10.1103/PhysRevB.79.125327 PACS number(s): 71.35.Pq, 75.50.Pp, 78.55.Et, 78.67.De

I. INTRODUCTION

Recent progress in quality of synthesized quantum structures in semiconductor materials has stimulated many interesting studies of the optical properties originated from a two-dimensional electron gas (2DEG). The optical response of 2DEG is well studied for two extreme cases: (1) when the photocreated excitons are completely screened and become nonradiative (a high-density limit),[1–11] and (2) when the density of the carriers (electrons or holes) is very low (a low-density limit). The first case occurs when the Fermi energy (E_F) is much larger than the exciton binding energy ($E_X^b < E_F$). In this case, the optical response is regarded as a perturbation of the Fermi sea caused by photocreated holes. The photoluminescence (PL) and absorption spectra are influenced by the many-body interactions of the excited quasiparticles at low temperatures.

In the second case when the excess carrier density is very low ($E_F \ll E_X^b$), the many-body effect and the screening effect mentioned above are suppressed. Excitonic effect becomes pronounced, and therefore, excitons and charged excitons appeared as discernible PL and as absorption peaks.[10–23] The negatively charged exciton consists of two electrons and one hole, and behaves like a hydrogen ion H^-. The negatively charged exciton recombines to emit one photon, leaving one electron in the conduction band. In a zinc-blende-type semiconductor, two singlet and six triplet charged excitons are considered to exist. The singlet charged exciton with $J = \pm 3/2$ and the triplet charged exciton with $J = \pm 1/2$ or $J = \pm 3/2$ are optically active. On the other hand, the triplet charged excitons with $J = \pm 5/2$ are the dark states, of which optical transition is forbidden. The charged excitons when subjected to the external magnetic field show much more complicated PL spectra than those of excitons. The optical properties of the charged excitons in an external magnetic field are much influenced by the spin states of the respective components (electrons and holes), and on the binding energy of the charged excitons. Therefore, several PL peaks of triplet charged excitons split by the Zeeman effect and increased binding energies of each charged exciton in magnetic fields were reported.[13,18–22] In a GaAs quantum well (QW), several PL lines of charged excitons were observed in high magnetic field, and the hidden crossover of a singlet and a dark triplet charged exciton was reported.[14,18–20] The dark states are not always optically forbidden.[16–21] In the above reports when both the "hidden symmetry" and the translational symmetry are broken in magnetic fields, the dark triplet charged exciton becomes optically active.[19–21] The breaking of the translational invariance, which was caused by disorders in quantum wells, relaxes the optical selection rules in magnetic fields. The hidden symmetry is broken by a Landau-level (LL) mixing, a valence-band mixing, and asymmetry of the quantum well in magnetic fields.

On the other hand, in case when the Fermi energy is between the binding energy of charged exciton and that of the exciton ($E_{X^-}^b < E_F < E_X^b$), it is reported that the PL spectra show both features of low and high electron-density states.[24–32] In this intermediate region of the electron density, the PL spectra in low magnetic fields ($\nu > 2$) show the Landau-level-like behavior[26,29] while in high magnetic fields ($\nu < 1$) the PL turns out to be a simple excitonic or charged excitonlike behavior.[26] When the filling factor becomes that between 1 and 2, the PL shows spectral features of both Landau-type and excitonic transitions. Therefore, in the magnetic field regimes of $\nu > 1$, the PL spectra in intermediate electron density are more complicated than those in both cases of low and high electron-density regions.[24–26,30–32]

Dilute magnetic semiconductors (DMS) such as (Cd,Mn)Te are known as a material in which the spin states of carriers are modified by the (s,p)-d exchange interaction between localized magnetic moments and free carriers in magnetic fields.[30–38] Therefore, the hidden singlet-triplet crossover of the charged excitons mentioned above in DMS QWs is expected to occur at much lower magnetic field than in nonmagnetic QWs. In our previous paper this crossover was observed around 1–2 T at 1.4 K.[30] The giant Zeeman splitting of the carriers can cause the complicated PL lines from the charged exciton transitions to be simpler with very

limited number of transition lines at very high magnetic fields. In (Cd,Mn)Te QWs, the sign of Lande's g factor of bare conduction electrons (g_e^*) and that of the effective g factor arising from s,p-d exchange interaction [$g_e^{s,p-d}(B,T)$] is opposite.[33,34] Therefore, a unique situation can be realized where the second hidden crossover of triplet to singlet charged exciton PL transitions occurs and the singlet charged exciton transition becomes the lowest energy on application of a very high magnetic field. In this paper, we study the PL spectra arising from charged excitons in n-doped $Cd_{1-x}Mn_xTe/Cd_{1-y}Mg_yTe$ QWs in high magnetic fields up to 140 T at low temperatures. Two well defined PL peaks and their hidden crossovers are observed in a wide range of magnetic field, and are assigned as the triplet and singlet charged exciton transitions. The conduction-electron g factor is shown to deduce from the two PL peak intensities.

II. SAMPLE AND EXPERIMENTS

The modulation n-doped $Cd_{1-x}Mn_xTe/Cd_{1-y}Mg_yTe$ (sample A: $x=0.018$, $y=0.147$, and sample B: $x=0.021$, $y=0.147$) single-quantum wells (the well width, $L_z=10$ nm, and the barrier width, $L_b=40$ nm) studied in this report was prepared by molecular-beam epitaxy and grown on a (001)-GaAs substrate. The electron density in both QWs is about $n=2\times10^{11}$ cm^{-2}, and the Fermi energy is about 4 meV. Sample A is the same sample whose absorption spectra are measured by Lemaître *et al.*[31] On the other hand, it is reported that the binding energy of singlet charged exciton in the CdTe QW at zero magnetic field are about 3 meV.[14] The binding energies in our sample have similar size to those in CdTe since Mn density is very low.

The PL spectra in magnetic fields were measured by two different systems. The first one is comprised of nondestructive pulse magnets and a polychromator equipped with an image intensifier-charge-coupled device array (I-CCD). The pulse width of nondestructive magnet is about 38 ms and the accessible maximum magnetic field is about 60 T. The optical detection was conducted with a streak mode, in which the optical spectra were recorded continuously with a scan of magnetic field. A single-turn coil system[39] was used for generation of magnetic fields up to 140 T. The pulse width of the magnetic field is about 8 μs.[40] Spectra are measured with the I-CCD at the flat top part of the pulsed magnetic field (about 1 μs). Samples are set in a liquid-He flow cryostat made of plastic materials.[41] Samples are mounted in the Faraday configuration in all the measurements.[42]

The right or left circularly polarized components of the PL spectra were chosen by a 1/4-λ plate and a linear polarizer. The samples were excited by an Ar^+ laser (514.5 nm) in the PL measurement. The excitation power was about 0.5 W cm^{-2} in the first and the second systems, and the laser power was restricted to be low so as to avoid an increase in temperature as well as the electron density. The excitation light was led to a sample in a cryostat by optical fibers and the PL from the sample was collected by the same optical fibers.

III. RESULTS AND DISCUSSION

Figure 1 shows the PL spectra in magnetic fields up to 60 T at temperature of 2 K measured for sample A ($x=0.018$).

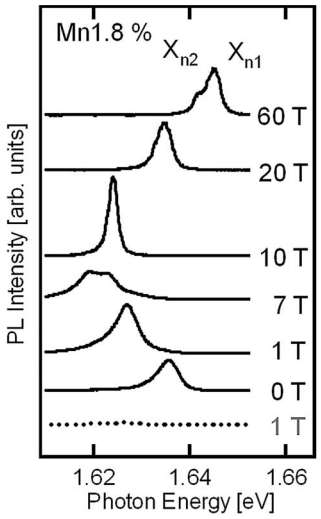

FIG. 1. PL spectra of the Mn 1.8% sample measured up to 60 T at 2 K. The solid and the dotted lines show the σ^+ and σ^- components of PL spectra, respectively.

The PL observed at 0 T is reported as arising from a singlet charged exciton (X_s^-).[30] The σ^- component of PL spectra is drastically suppressed by increasing magnetic field and finally vanishes above 1 T. The σ^+ component exhibits a drastic change with large energy shifts and appearance of several new peaks below 10 T, of which details were presented in our paper.[30] Almost all of the peaks vanish above 10 T and a sharp PL peak (X_{n1}), which appears about 5 T, emits strong luminescence from 10 to 60 T. A new peak (X_{n2}) below X_{n1} PL peak appears above 50 T and its intensity grows gradually with increasing magnetic field. Overall behavior of the spectra in sample B ($x=0.021$) is similar. The PL intensity of X_{n2} in sample A is stronger than that in sample B at 60 T, showing a slight Mn concentration dependence of X_{n2} peak.

Figure 2 shows a streak image of PL in magnetic fields. In Fig. 2(a), the PL of X_{n2} at 2 K starts to appear above 50 T. The X_{n2} PL peak, which is located at the lower energy side of X_{n1} peak, becomes strong with increasing temperature as shown in Fig. 2(b). This fact indicates that the initial state of X_{n2} PL transition should be located at a higher energy side than that of X_{n1} as shown in the inset.

The initial states of X_{n1} and X_{n2} are assigned as the triplet charged exciton with $J=+1/2$ [$X_t^-(+1/2)$] and the singlet charged exciton with $J=+3/2$ [$X_s^-(+3/2)$], respectively. This assignment is justified in the Appendix. In order to understand the PL behavior of charged excitons in magnetic fields, we calculated the energy states of $X_s^-(+3/2)$, $X_t^-(+1/2)$, and dark triplet charge exciton with $J=+5/2$ [$X_{td}^-(+5/2)$] in (Cd,Mn)Te/(Cd,Mg)Te. The energy states of charged excitons in dilute magnetic semiconductors subjected to a magnetic field is given by

$$E(B,T) = E_g(T) + E^b(B) + E^Z(B,T) + E^{LL}(B,T), \qquad (1)$$

where $E_g(T)$ is the band gap and $E^b(B)$ is a binding energy of a charged exciton added with that of an exciton. $E^Z(B)$ is a Zeeman energy of charged excitons. $E^{LL}(B,T)$ is the LL energy. In Eq. (1), $E^b(B)$ is an unknown value but the energy

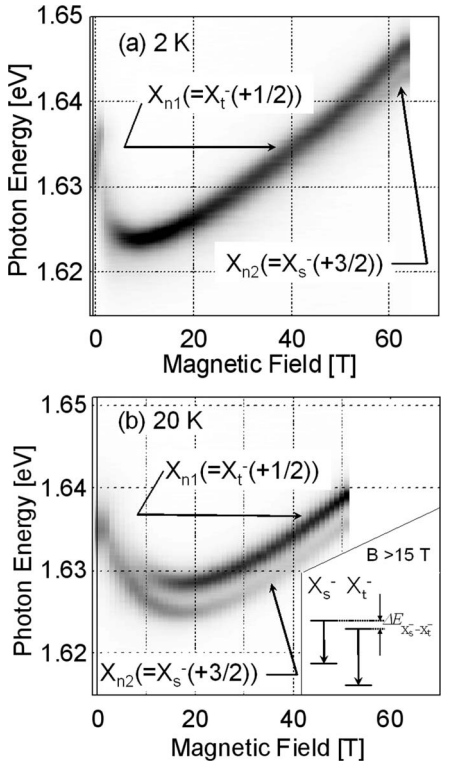

FIG. 2. The streak image of PL spectra of sample A in magnetic fields at (a) 2 and (b) 20 K. The inset shows the proposed transition diagram of X_{n1} and X_{n2}.

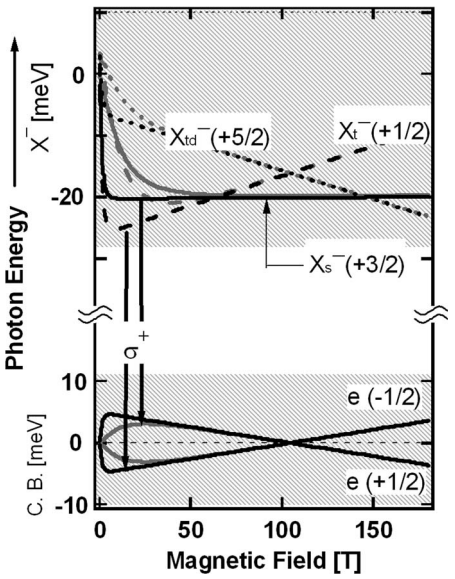

FIG. 3. The transition diagram of charged excitons that is estimated by a simple model in magnetic fields. The gray and the black lines are the energy states at 20 and 2 K, respectively. The lower solid lines are the energy states of conduction electrons of $J=+1/2$ and of $J=-1/2$. The higher solid line shows the spin splitting state of $X_s^-(+3/2)$. The broken and the dotted lines show the spin splitting states of $X_t^-(+1/2)$ and $X_{td}^-(+5/2)$, respectively.

difference between singlet and triplet charged excitons, which is equal to the energy difference between X_{n1} and X_{n2} peaks as discussed in the Appendix, can be estimated as about 3.5 meV between 10–50 T at 20 K as shown in Fig. 2. We take account of both the Zeeman energy of (s,p)-d exchange interaction and the Zeeman energy determined by Landé g factor of bear electrons and holes, and $E^Z_{X_s^-}(B,T)$, $E^Z_{X_t^-}(B,T)$, and $E^Z_{X_{td}^-}(B,T)$, are given by

$$E^Z_{X_s^-(\pm 3/2)}(B,T) = \pm \frac{1}{2} x N_0 \beta S_0 B_s\left(\frac{g_{\mathrm{Mn}}\mu_B SB}{k_B T}\right) \mp \frac{g_h^* \mu_B B}{2}, \tag{2}$$

$$E^Z_{X_t^-(\pm 1/2)}(B,T) = \pm \frac{1}{2} x N_0 (2\alpha - \beta) S_0 B_s\left(\frac{g_{\mathrm{Mn}}\mu_B SB}{k_B T}\right) \pm \frac{(2g_e^* + g_h^*)\mu_B B}{2}, \tag{3}$$

$$E^Z_{X_{td}^-(\pm 5/2)}(B,T) = \pm \frac{1}{2} x N_0 (2\alpha + \beta) S_0 B_s\left(\frac{g_{\mathrm{Mn}}\mu_B SB}{k_B T}\right) \pm \frac{(2g_e^* - g_h^*)\mu_B B}{2}, \tag{4}$$

where B_s is the Brillouin function. $N_0\alpha$ and $N_0\beta$ denote the s,p-d exchange constants, and are given by $N_0\alpha=0.22$ (eV), $N_0\beta=0.88$ (eV), and $g_{\mathrm{Mn}}=2$, $S=5/2$ in CdMnTe. X is the Mn concentration and S_0 is the effective spin of Mn. Here, $S_0=5/2$ since Mn concentration is very low. g_e^* is equal to -1.64 taken from the bulk CdTe.[43] The absolute value of g_h^* in CdTe QWs is set to zero.[14]

In Eq. (1), $E^{LL}(B,T)$ is written by $E^{LL}(B,T)=(n+1/2)\cdot\hbar\omega$, with $\omega=eB(1/m_e+1/m_h)$, where m_e and m_h are the cyclotron mass of an electron and a hole. $m_e=0.105m_0$ and $m_h=0.193m_0$ are the values estimated by Lemaître *et al.*[31] The lowest LL energy takes the same value irrespective of the sort of charged excitons. Moreover the binding-energy difference between $X_s^-(+3/2)$ and $X_t^-(+1/2)$ $[\Delta E^b_{X_s^- - X_t^-}(B)]$ is almost constant in magnetic field under consideration as shown in Fig. 2. Therefore, the PL behavior is mostly determined by the Zeeman term of charged excitons.

Figure 3 shows the spin splittings of charged excitons and conduction electrons in magnetic fields, which are calculated by the parameters for sample A but with an assumption of a constant energy of both the binding energy of $X_t^-(+1/2)$ $[E^b_{X_t^-}(B)]$ and $X_t^-(+5/2)$ $[E^b_{X_{td}^-}(B)]$. This assumption is invalid in a region of low magnetic fields[14] but this assumption can be applied at high magnetic fields. At 2 K, the energy splitting arising from the s,p-d exchange interaction is already saturated at 7 T. The initial energy difference between $X_s^-(+3/2)$ and $X_t^-(+1/2)$ $[\Delta E_{X_s^- - X_t^-}(B)]$ becomes maximum around 5 T, and decreases gradually with increasing magnetic field due to the negative contribution of g_e^*. Thereby, a second hidden triplet-singlet crossover between $X_s^-(+3/2)$ and $X_t^-(+1/2)$ is expected to occur around 65 T.

An increasing temperature reduces the s,p-d exchange interaction mentioned above. $\Delta E_{X_s^- - X_t^-}(B)$ below 50 T at 20 K becomes smaller than that at 2 K as shown in Fig. 3. Hence,

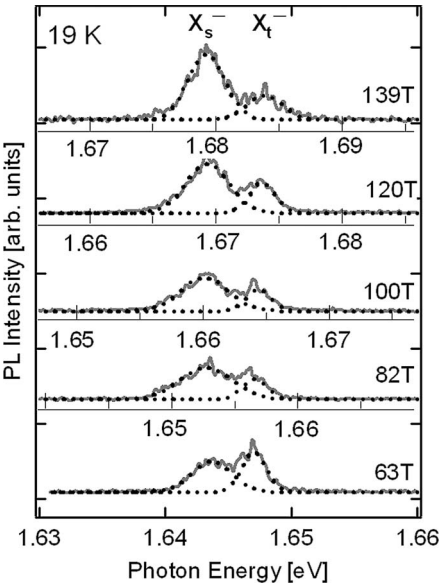

FIG. 4. The PL spectra in high magnetic fields above 60 T and temperature at 20 K. The dashed lines show the deconvoluted lines by a Gaussian function. The abscissa axis of each spectra are shifted to assist for comparing $X_s^-(+3/2)$ to $X_t^-(+1/2)$.

a number of $X_s^-(+3/2)$ states increases with increasing temperature, and as a result, the PL of $X_s^-(+3/2)$ becomes stronger as shown in Fig. 2(b). On the other hand, the lower energy shift of $X_{td}^-(+5/2)$ state is increased with increasing magnetic field. Then, the hidden singlet-dark triplet crossover between $X_{td}^-(+5/2)$ and $X_s^-(+3/2)$ should occur around 150 T, if assuming $X_{td}^-(+5/2)$ as $\Delta E_{X_{td}^-}^b(B) = \Delta E_{X_t^-}^b(B)$ in the magnetic field. However, it is reported that $\Delta E_{X_{td}^-}^b(B) > \Delta E_{X_t^-}^b(B)$.[14] In this case, the hidden singlet-dark triplet crossover can take place at a field lower than 150 T and appearance of the PL of $X_{td}^-(+5/2)$ is expected as reported in CdTe quantum wells.[14]

In order to study the hidden triplet-singlet crossover in high magnetic fields, we measure the PL spectra which were conducted by the single-turn coil above 60–140 T. Figure 4 shows the results at 20 K. As seen in Fig. 4, the PL intensity of $X_s^-(+3/2)$ grows with increasing magnetic field, and overcomes that of $X_t^-(+1/2)$ at a magnetic field between 63 and 82 T. This fact is considered to be caused by the second hidden triplet-singlet crossover between $X_s^-(+3/2)$ and $X_t^-(+1/2)$ at this field region. The energy difference between the two PL peaks related to $\Delta E_{X_s^- - X_t^-}^b(B)$ described above is still constant (about 3.5 meV) over the magnetic fields up to 140 T. On the other hand, the PL peaks of $X_{td}^-(+5/2)$ is not observed in this magnetic field region. The PL of $X_{td}^-(+5/2)$ can be observed in quantum wells with interface disorders.[22] The fact that the PL peak of $X_{td}^-(+5/2)$ is missing indicates that the hidden singlet-dark triplet crossover mentioned above cannot be realized in this field range.

The PL intensity of charged excitons in general reflects initial energy states of the optical transitions. Figure 5(a) shows the intensity ratio of the $X_t^-(+1/2)$ PL against that of total PL $[\Gamma = I_{X_t^-}/(I_{X_t^-} + I_{X_s^-})]$ in magnetic fields. The open and

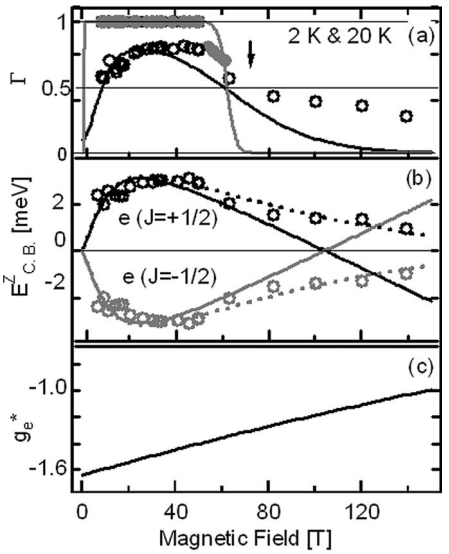

FIG. 5. (a) The intensity ratio (Γ) of the $X_t^-(+1/2)$ PL against that of the total PL up to 140 T at 2 (gray) and at 20 K (black). Circles are from experimental. Lines are calculated. (b) The spin splitting of conduction electrons. The black and the gray solid lines show the calculated energy states of $J=+1/2$ and of $J=-1/2$, respectively. The open circles are the experimental values. The dashed lines show the fitting lines which take into account the increase in the Lande's g factor in magnetic fields. (c) The value of the conduction-electron g factor estimated from the fitting lines (dashed lines) in (b).

closed circles are the experimental values at 20 and 2 K. At 20 K, Γ increases gradually up to 50 T, and then starts to decrease with increasing magnetic field. The ratio becomes closer to 1/2 at around 75 T, and tends to decrease further up to the highest magnetic field. The number of charged excitons is determined by a Boltzmann distribution under steady-state photoexcitation. The PL intensity of charge excitons is obtained by number of carriers and decay time (τ). Therefore Γ is given by

$$\Gamma = 1/[1 + (\tau_{X_t^-}/\tau_{X_s^-})\exp(-\beta \Delta E_{X_s^- - X_t^-})], \tag{5}$$

$\tau_{X_s^-}$ and $\tau_{X_t^-}$ are the decay times of $X_s^-(+3/2)$ and $X_t^-(+1/2)$, respectively. One assumes here $(\tau_{X_t^-}/\tau_{X_s^-} \approx 1)$ inferred from an analogy of the previous report,[30] and then the solid (gray and black) lines in Fig. 5(a) are obtained from Eq. (5) with the values $\Delta E_{X_s^- - X_t^-}$ calculated in Fig. 3. The calculated lines are roughly coincident with experimental ones up to 40 T at both temperatures. However, the calculated values are suppressed at lower magnetic fields than those of the experiment above 40 T at 20 K. This fact indicates that the experimental values of $\Delta E_{X_s^- - X_t^-}(B)$ should be much smaller than those of calculation at such high magnetic fields.

In the present case, $\Delta E_{X_s^- - X_t^-}(B)$ is shown to be determined by the Zeeman splitting of the conduction electrons as follows. The optical transitions of $X_t^-(+1/2)$ and $X_s^-(+3/2)$ are described by

$$X_s^-(e\downarrow e\uparrow h\uparrow) \rightarrow \hbar\omega_{X_s^-} + e\uparrow, \tag{6}$$

$$X_t^-(e\downarrow e\downarrow h\uparrow) \rightarrow \hbar\omega_{X_t^-} + e\downarrow, \tag{7}$$

respectively. $e\uparrow$ and $e\downarrow$ show the energy states of the conduction band with $J=+1/2$ and $J=-1/2$. Subtracting Eq. (7) from Eq. (6), one obtains

$$\Delta E_{X_s^- - X_t^-}(B) + \Delta E^b_{X_s^- - X_t^-}(B) = e\uparrow - e\downarrow = E^Z_{\mathrm{CB}}(B), \tag{8}$$

where $\Delta E_{X_s^- - X_t^-}(B)$ is the initial energy difference between $X_s^-(+3/2)$ and $X_t^-(+1/2)$ defined before. In the right-hand side, $\hbar\omega_{X_t^-} - \hbar\omega_{X_s^-}$ is equal to $\Delta E^b_{X_s^- - X_t^-}(B)=3.5$ meV as has been mentioned before, and $e\uparrow - e\downarrow$ corresponds to the Zeeman splitting energy of the conduction band, denoted by $E^Z_{\mathrm{CB}}(B)$.

The Zeeman splitting energies of the conduction band in magnetic fields at 20 K are shown in Fig. 5(b). The open circles are the values evaluated from the experimental values at 20 K (open circles) in Fig. 5(a) by use of Eqs. (5) and (8). The solid lines are the results of calculation in Fig. 3. The dashed lines are the result of fitting of the values deduced from experimental ones (open circles). Above 60 T, the experimental values behave quite differently from the calculated solid lines which show a linear dependence on magnetic field and crosses each other around 100 T. The rate of decrease in observed Zeeman splitting is suppressed on increasing magnetic field, and the spin crossover between $J=+1/2$ and $J=-1/2$ states in conduction electrons cannot be realized until 140 T. The discrepancy between experiment and calculation is considered to arise from a nonmonotonous magnetic field dependence of the conduction-electron bare Lande's g factor.

Figure 5(c) shows the magnetic field dependence of bare Lande's g factor of conduction electrons estimated from the dotted lines which are fitted to the experimental data in Fig. 5(b). The bare Lande's g factor increases almost linearly from −1.64 to −1.0 in magnetic fields between 0 and 140 T (0.0046 /T). Similar behavior was reported in bulk GaAs studied by cyclotron measurements in high magnetic fields, where the bare electron g factor varies from −0.44 to 0 up to 100 T (0.0044 /T), and the change was explained by the nonparabolicity of the conduction band.[44]

The increase in bare Lande's g factor of conduction electrons also results in the increased magnetic field, at which the second hidden triplet-singlet crossover between $X_t^-(+1/2)$ and $X_s^-(+3/2)$, or singlet-dark triplet between $X_s^-(+3/2)$ and $X_{td}^-(-5/2)$ takes place, can explain the PL behavior of charged excitons in high magnetic fields as shown in Figs. 2 and 4.

IV. CONCLUSION

We studied the two-dimensional charged excitons realized in dilute magnetic semiconductor quantum wells (Cd,Mn)Te/(Cd,Mg)Te. We have observed the PL spectra arising from the charged excitons at low temperature in high magnetic fields up to 140 T. The two dominant PL peaks are observed above 10 T, and we assigned the lower peak to $X_s^-(+3/2)$ and the higher peak to $X_t^-(+1/2)$. It was shown from our PL analysis that the second hidden singlet-triplet crossover between $X_t^-(+1/2)$ and $X_s^-(+3/2)$ took place between 63 and 82 T at 20 K. It was found that the PL behaviors of charged excitons in high magnetic fields are determined by those of the bare electron Lande's g factor. In our case, the bare Lande's g factor of the conduction electrons is successfully derived from the PL intensity analysis of the charged excitons in magnetic fields.

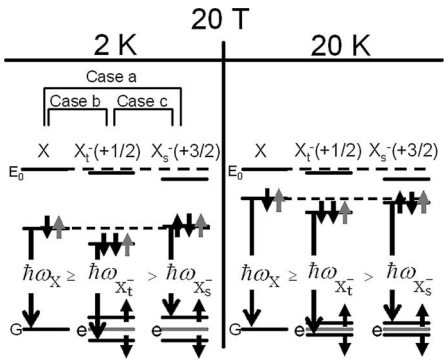

FIG. 6. The transition diagram of $X_s^-(+3/2)$, $X_t^-(+1/2)$, and $X(+1)$ expected at about 20 T. The black and gray short arrows show the up-spin and down-spin states of electrons and holes, respectively.

ACKNOWLEDGMENTS

This work was partially supported by a Grant-in-Aid for Scientific Research on Priority Area "High Field Spin Science in 100 T" (Grant No. 451) from the Ministry of Education, Culture, Sports, Science, and Technology (MEXT) of Japan.

APPENDIX: IDENTIFICATION OF PL PEAKS IN HIGH MAGNETIC FIELDS

In order to clarify the origin of the two PL peaks (X_{n1}, X_{n2}) in magnetic fields as shown in Fig. 2, we argue the following four possibilities. In the first case [interband Landau level transitions (ILLT) and the charged exciton], the ILLT transitions are observed even in low magnetic fields, in the case when the electron density is high. However, it is reported that the PL or absorption spectra change from ILLT to excitonic transition above a critical magnetic field $(\nu<2)$.[25] In our sample, the magnetic field of $\nu=2$ changes already at about 4.7 T.[30] Additionally, the spectral shapes of both PL peaks are sharp, showing typical of the excitonic transition.

In the second case (excitons and biexcitons), the PL peak of a biexciton can appear at the lower energy side of that of an exciton. However, a biexciton cannot be formed in such high magnetic field due to the same reason discussed in Ref. 45.

In the third case {in the case of excitons with $J=+1$ $[X(+1)]$ for X_{n1} and the charged excitons for X_{n2}}, the charged exciton transition should arise from $X_s^-(+3/2)$ or $X_t^-(+1/2)$. As illustrated in Fig. 6 (case a) for instance at 20 T, the exciton PL photon energy $(\hbar\omega_X)$ should be larger than that of a $X_s^-(+3/2)$ $(\hbar\omega_{X_s^-})$ by an amount of the charged ex-

citon binding energy ($E^b_{X^-_s}$) since the total Zeeman energies of the initial and final states for both cases are the same. The amount of lower energy shifts due to the Zeeman splittings are estimated from Fig. 2(a), for $X(+1)$ and $X^-_s(+3/2)$, and are about 19 and 15 meV, respectively, at 2 K and 20 T. The energy difference between X_{n1} and X_{n2} peaks is about 3.5 meV at 20 K as shown Fig. 2(b), which should correspond to $E^b_{X^-_s}$, and comparable to the energy difference of the lower energy shifts between the two states. Hence, the lowest energy of the initial state is almost the $X(+1)$ and $X^-_s(+3/2)$ as illustrated in Fig. 6. In this case, two peaks should appear in Fig. 2(a), whereas only one peak is observed. The Zeeman splittings become smaller with increasing temperature, and, for example, at 20 K, the difference of the Zeeman shifts for both states becomes smaller than $E^b_{X^-_s}$. Henceforth, the charged excitons remain as the lower energy state than that of the exciton (Fig. 6 at 20 K). This fact should show up as a stronger PL of the charged exciton than that of the exciton, which contradicts with the behavior of X_{n1} and X_{n2} peaks in Fig. 2(b).

We consider the next case when X_{n2} arise from $X^-_t(+1/2)$ as illustrated in Fig. 6 (case b). The photon energy of the X^-_t PL ($\hbar\omega_{X^-_t}$) is always smaller than the $\hbar\omega_X$ by the amount of $X^-_t(+1/2)$ binding energy ($E^b_{X^-_t}$), and the amount of the Zeeman shift of $X^-_t(+1/2)$ ($E^Z_{X^-_t}$) is much larger than that of $X(+1)$ (E^Z_X) in magnetic fields. In this case as shown in Fig. 6, the initial state of $X^-_t(+1/2)$ is much lower in energy than that of $X(+1)$. Therefore, at 2 K, the only PL of $X^-_t(+1/2)$ should be observable as the lower energy peak (X_{n2}), which does not explain the domination of X_{n1} as seen in Fig. 2(a).

In the third case [$X_{n1}=X^-_t(+1/2), X_{n2}=X^-_s(+3/2)$], as illustrated in Fig. 6 (case c), $\hbar\omega_{X^-_s}$ is lower than $\hbar\omega_{X^-_t}$ by an energy value of $\Delta E^b_{X^-_s-X^-_t}$ (the energy difference between $E^b_{X^-_s}$ and $E^b_{X^-_t}$). The amount of $E^Z_{X^-_t}$ is larger than that of $E^Z_{X^-_s}$ by $2|E^Z_e|$. At 2 K, the energy difference between $E^Z_{X^-_s}$ and $E^Z_{X^-_t}$ at 20 T is estimated as about 8 meV and is much larger than $\Delta E^b_{X^-_s-X^-_t}$ which is about 3.5 meV as shown in Fig. 2. Therefore the initial state of $X^-_t(+1/2)$ is much lower than that of $X^-_s(+3/2)$. Then, the transition of $X^-_t(+1/2)$ is expected as the dominant PL observed at 2 K. The Zeeman splittings arising from the s,p-d exchange interaction decreases with increasing temperature. Therefore, at 20 K, the energy difference of lowest sates for both $X^-_s(+3/2)$ and $X^-_t(+1/2)$ approaches zero, and the PL from $X^-_s(+3/2)$ is observed in addition to $X^-_t(+1/2)$ PL. The fourth model can only explain the behavior of two PL peaks in Fig. 2.

[1] Y. I. Mazur, G. G. Tarasov, Z. Y. Zhuchenko, H. Kissel, U. Muller, V. P. Kunets, and W. T. Masselink, Phys. Rev. B **66**, 035308 (2002).

[2] M. S. Skolnick, J. M. Rorison, K. J. Nash, D. J. Mowbray, P. R. Tapster, S. J. Bass, and A. D. Pitt, Phys. Rev. Lett. **58**, 2130 (1987).

[3] V. Huard, R. T. Cox, K. Saminadayar, A. Arnoult, and S. Tatarenko, Phys. Rev. Lett. **84**, 187 (2000).

[4] Y. Iwasa, J. S. Lee, and N. Miura, Solid State Commun. **64**, 597 (1987).

[5] M. Potemski, Physica B **256-258**, 283 (1998).

[6] T. B. Kehoe, C. M. Townsley, A. Usher, M. Henini, and G. Hill, Phys. Rev. B **68**, 045325 (2003).

[7] K. Asano and T. Ando, Phys. Rev. B **65**, 115330 (2002).

[8] F. J. Teran, Y. Chen, M. Potemski, T. Wojtowicz, and G. Karczewski, Phys. Rev. B **73**, 115336 (2006).

[9] S. Schmitt-Rink, C. Ell, S. W. Koch, H. E. Schmidt, and H. Haug, Solid State Commun. **52**, 123 (1984).

[10] K. Kheng, R. T. Cox, Y. MerledAubigné, F. Bassani, K. Saminadayar, and S. Tatarenko, Phys. Rev. Lett. **71**, 1752 (1993).

[11] A. S. Bracker, E. A. Stinaff, D. Gammon, M. E. Ware, J. G. Tischler, D. Park, D. Gershoni, A. V. Filinov, M. Bonitz, F. M. Peeters, and C. Riva, Phys. Rev. B **72**, 035332 (2005).

[12] D. Andronikov, V. Kochereshko, and A. Platonov, T. Barrick, S. A. Crooker, and G. Karczewski, Phys. Rev. B **72**, 165339 (2005).

[13] C. Schüller, K.-B. Broocks, P. Schröter, Ch. Heyn, D. Heitmann, M. Bichler, W. Wegscheider, T. Chakraborty, and V. M. Apalkov, Phys. Rev. Lett. **91**, 116403 (2003).

[14] G. V. Astakhov, D. R. Yakovlev, V. V. Rudenkov, P. C. M. Christianen, T. Barrick, S. A. Crooker, A. B. Dzyubenko, W. Ossau, J. C. Maan, G. Karczewski, and T. Wojtowicz, Phys. Rev. B **71**, 201312(R) (2005).

[15] M. Byszewski, B. Chwalisz, D. K. Maude, M. L. Sadowski, M. Potemski, T. Saku, Y. Hirayama, S. Studenikin, D. G. Austing, A. S. Sachrajda, and P. Hawrylak, Nat. Phys. **2**, 239 (2006).

[16] M. A. Lampert, Phys. Rev. Lett. **1**, 450 (1958).

[17] A. Gładysiewicz, L. Bryja, A. Wójs, and M. Potemski, Phys. Rev. B **74**, 115332 (2006).

[18] F. M. Munteanu, D. G. Rickel, C. H. Perry, Y. Kim, J. A. Simmons, and J. L. Reno, Phys. Rev. B **62**, 16835 (2000).

[19] G. Yusa, H. Shtrikman, and I. Bar-Joseph, Phys. Rev. Lett. **87**, 216402 (2001).

[20] C. Schüller, K.-B. Broocks, Ch. Heyn, and D. Heitmann, Phys. Rev. B **65**, 081301(R) (2002).

[21] D. M. Whittaker and A. J. Shields, Phys. Rev. B **56**, 15185 (1997).

[22] A. Wójs, J. J. Quinn, and P. Hawrylak, Phys. Rev. B **62**, 4630 (2000).

[23] T. Vanhoucke, M. Hayne, M. Henini, and V. V. Moshchalkov, Phys. Rev. B **63**, 125331 (2001).

[24] B. M. Ashkinadze, E. Linder, E. Cohen, A. B. Dzyubenko, and L. N. Pfeiffer, Phys. Rev. B **69**, 115303 (2004).

[25] D. Sanvitto, R. A. Hogg, A. J. Shields, D. M. Whittaker, M. Y. Simmons, D. A. Ritchie, and M. Pepper, Phys. Rev. B **62**, R13294 (2000).

[26] D. Keller, D. R. Yakovlev, G. V. Astakhov, W. Ossau, S. A. Crooker, T. Slobodskyy, A. Waag, G. Schmidt, and L. W. Mo-

lenkamp, Phys. Rev. B **72**, 235306 (2005).
[27] W. Ossau, V. P. Kochereshko, G. V. Astakhov, D. R. Yakovlev, G. Landwehr, T. Wojtowicz, G. Karczewski, and J. Kossut, Physica B **298**, 315 (2001).
[28] G. Finkelstein, H. Shtrikman, and I. Bar-Joseph, Phys. Rev. B **53**, 12593 (1996).
[29] E. I. Rashba and M. D. Sturge, Phys. Rev. B **63**, 045305 (2000).
[30] Y. Hirayama, H. Yamamoto, H. Mino, S. Takeyama, G. Karczewski, T. Wojtowicz, and J. Kossut, Physica E (Amsterdam) **22**, 620 (2004).
[31] A. Lemaître, C. Testelin, C. Rigaux, T. Wojtowicz, and G. Karczewski, Phys. Rev. B **62**, 5059 (2000).
[32] F. J. Teran, M. L. Sadowski, M. Potemski, G. Karczewski, S. Mackowski, and J. Jaroszynski, Physica B **256-258**, 577 (1998).
[33] F. J. Teran, M. Potemski, D. K. Maude, T. Andrearczyk, J. Jaroszynski, and G. Karczewski, Phys. Rev. Lett. **88**, 186803 (2002).
[34] T. Wojtowicz, M. Kutrowski, G. Karczewski, J. Kossut, F. J. Teran, and M. Potemski, Phys. Rev. B **59**, R10437 (1999).
[35] F. Takano, H. Akinaga, T. Tokizaki, S. Kuroda, and K. Takita, Appl. Phys. Lett. **83**, 2853 (2003).
[36] H. Yokoi, Y. Kakudatea, K. Uchida, S. Takeyama, N. Miura, Y. Kim, G. Karczewski, T. Wojtowicz, and J. Kossut, Physica E (Amsterdam) **22**, 636 (2004).
[37] T. Wojtowicz, M. Kutrowski, G. Karczewski, and J. Kossut, Appl. Phys. Lett. **73**, 1379 (1998).
[38] Y. Imanaka, T. Takamasu, G. Kido, G. Karczewski, T. Wojtowicz, and J. Kossut, Microelectron. Eng. **63**, 69 (2002).
[39] K. Nakao, F. Herlach, T. Goto, S. Takeyama, T. Sakakibara, and M. Miura, J. Phys. E **18**, 1018 (1985).
[40] N. Miura, T. Osada, and S. Takeyama, J. Low Temp. Phys. **133**, 139 (2003).
[41] S. Takeyama, M. Kobayashi, A. Matsui, K. Mizuno, and N. Miura, *High Magnetic Fields in Semiconductor Physics*, edited by G. Landwehr, Springer Series in Solid-State Sciences (Springer, Berlin, 1987), p. 555.
[42] S. Takeyama, K. Watanabe, N. Miura, T. Komatsu, K. Koike, and Y. Kaifu, Phys. Rev. B **41**, 4513 (1990).
[43] M. Willatzen, M. Cardona, and N. E. Christensen, Phys. Rev. B **51**, 17992 (1995).
[44] S. P. Najda, S. Takeyama, N. Miura, P. Pfeffer, and W. Zawadzki, Phys. Rev. B **40**, 6189 (1989).
[45] S. Takeyama, Y. Natori, Y. Hirayama, E. Kojima, Y. Arisima, H. Mino, G. Karczewski, T. Wojtowicz, and J. Kossut, J. Phys. Soc. Jpn. **77**, 044702 (2008).